

Development and Analysis of Innovative Nano-fillers Derived from Groundnut Shell for Enhanced Polymer Composites

*Nworie Cyril Emeka, Ochi Daniel Okey, Umar Ahmed Gana, Aliu Salisu Otsekhai,

Atulute Oluwasegun O.

Department of Chemical Engineering Technology, Auchi Polytechnic, Auchi, Nigeria

*Corresponding Author: nocyka2016@gmail.com

Accepted: May 5, 2026. **Published Online:** May 8, 2026

ABSTRACT

This research focused on the development and characterization of nanofillers prepared from groundnut shells for enhanced polymer composites. The shells were sun-dried and ground using a grinding mill. The resulting material was sieved through a 0.150 mm mesh, and subjected to ball milling to achieve a particle size of 96 nm. The nanofillers made from groundnut shells were added to polymer matrices with loadings varying from 10 to 50 g to assess their reinforcing capabilities. Mechanical tests indicated that a loading of 30 g provided the best results, with tensile strength reaching 15.99 N/mm², an increase in Shore A hardness by 57%, and a reduction in compression set by 27%. At a loading of 40 g, there was improvement in abrasion resistance, while flex fatigue performance improved with increased nanofiller content. It peaked at 4,442 cycles with a 50 g loading. SEM/EDX analysis showed microstructures, whereas FTIR spectroscopy identified functional groups, such as hydroxyl groups (3411.23 cm⁻¹), cellulosic elements (1050.28 cm⁻¹), and lignin-related functionalities (2250.19 cm⁻¹). XRD analysis indicated high crystallinity, with a prominent reflection observed at $2\theta = 43^\circ$. These nanofillers showed considerable promise as sustainable reinforcement materials for polymer composites in applications.

Keywords: Nanofillers, characterization, polymer composites, groundnut shells, agricultural waste

INTRODUCTION

The emergence of sustainable materials has garnered significant interest due to ecological issues and the rising demand for high-performance polymer composites [1]. The growing reliance on synthetic fillers in polymer composites raises both environmental and economic concerns. Traditional fillers, like carbon black and silica, are not renewable, costly, and may present health hazards [2]. Furthermore, agricultural by-products are frequently discarded or incinerated,

resulting in pollution and wasted resources [3]. Consequently, there is a pressing need for alternative, sustainable fillers that provide similar or enhanced performance while minimizing environmental impact.

A significant breakthrough in this area is the integration of nanofillers into polymer matrices to improve mechanical, thermal, and barrier characteristics [4]. Organic waste materials, like agricultural by-products, have become promising candidates for sustainable nanofillers because of their availability, renewability, and ability to decompose [5].

Groundnut (*Citrullus colocynthis*) shell, which is often overlooked as an agro-waste, offers a promising source for producing nanofillers. Abundant in cellulose, lignin, and other structural elements, Groundnut shell can be transformed into nanofillers using mechanical, chemical, and thermal processes [6]. When these nanofillers are integrated into polymer matrices, they can enhance properties such as strength, durability, and biodegradability, making them viable for various applications, including packaging, automotive components, and biomedical devices [7].

This research examines the development and characterization of innovative nanofillers obtained from groundnut shells and their prospective use in enhanced polymer composites. The objective of the study is to investigate environmentally friendly methods for repurposing agricultural waste while enhancing the properties of polymer materials.

MATERIALS AND METHODS

Collection of groundnut shell

Groundnut shells (Plate 1) were gathered from processing locations in Okpella, Edo State, Nigeria. To eliminate any attached impurities and soluble organic materials, the shells were immersed in clean water for a duration of three days. After this pre-treatment, the shells were washed, drained, and left to sun dry, then coarsely ground using a grinding machine to achieve a consistent feedstock for subsequent processing.



Plate 1: Samples of groundnut shell

Pulverization of groundnut shell

The blended shells underwent an oven drying process at 120°C for 1 hour to diminish moisture content, followed by pulverization with a Tigmax petrol engine – Gx 160- 5.5 Hp grinding mill. This step of pulverization was crucial for breaking the shell structure into fine particles, which enhances the surface area for better interaction with the polymer matrix (Plate 2). The material was then sieved to a mesh size of 0.150 μm and processed in a planetary ball mill (Retsch PM 400) for 2 hours at 300 rpm to achieve particles measuring 96 nm, ensuring uniformity for further characterization and the formulation of composites.



Plate 2: Prepared samples of groundnut shell (pulverized samples)

Compounding of rubber

The formulation of rubber composites was conducted using a two-roll mill (Plate 3). A total of 500 g of natural rubber was masticated until softened, after which processing oil was gradually introduced to enhance mixing. Sequential incorporation of compounding agents was carried out, beginning with 20g of zinc oxide, 10g of stearic acid, 6g of accelerator, and a measured quantity of TMQ. Thereafter, nanofillers derived from groundnut shell were incorporated at varying loadings of 10, 20, 30, 40, and 50g, followed by the addition of 10g of sulphur to serve as a

vulcanizing agent. Continuous mixing was maintained until a homogenous composite material was obtained.



Plate 3: Compounding machine

The 20 g of nanofillers with 10 g of sulphur were also added until a uniform material was formed. The same step was repeated for 10 g, 30 g, 40 g and 50 of nanofillers

Vulcanizing of rubber

The compounded materials were molded and subjected to vulcanization using a 25-ton hydraulic press (Plate 4). The samples were placed on mold to allow free air to escape, after which the press was operated at a set temperature of 150°C for 45 minutes. The process facilitated the crosslinking between Sulphur and rubber chains.



Plate 4: Vulcanized rubber

Characterization of nanofiller

The size of the nanofillers was determined using a mesh with a 0.150 mm opening, revealing a particle size of 96 nm obtained through ball milling. The bulk density of the sample was determined via the tapping method. The moisture content was assessed by drying the blended groundnut shell powder until it achieved a consistent weight. The pH of the powdered sample was measured by combining 1.0 g of the sample with 10.0 mL of deionized water in a 50 mL beaker.

Characterization of composites

To evaluate the structural and chemical interactions within the nanofiller–rubber composites, morphological and spectroscopic analyses were carried out.

These include Tensile strength analysis, Hardness determination, Abrasion test, Compression test, Flex fatigue test, Optimal loading determination and Reinforcement tests which were conducted according to standard methods.

Scanning Electron Microscopy (SEM) analysis

The surface structure of the vulcanized composites was analyzed using Scanning Electron Microscopy. Small pieces of the rubber samples were sliced, affixed to aluminum stubs, and coated with a fine layer of gold to enhance surface conductivity. The samples that were prepared were subsequently placed in the SEM chamber, where a focused electron beam was directed across the surface.

Fourier Transform Infrared Spectroscopy

The chemical interactions between the nanofillers from groundnut shells and the polymer matrix were evaluated using Fourier Transform Infrared Spectroscopy. Composite samples that were finely ground were examined in the mid-infrared range ($4000\text{--}400\text{ cm}^{-1}$). Infrared radiation was directed through the samples, and the absorbance patterns were documented as spectra.

X-Ray Diffraction

The crystalline structure and phase composition of the composites were examined using X-ray diffraction. The vulcanized samples were prepared as flat sections and exposed to monochromatic X-rays.

RESULTS AND DISCUSSION

Tensile strength analysis

The original tensile strength data from this study show a non-linear relationship with nanofiller loading. Sample A (10 g) exhibited the lowest tensile strength of 12.62 N/mm^2 , while Sample C (30 g) achieved the highest value of 15.99 N/mm^2 , a 27% improvement over the baseline formulation. This enhancement is consistent with findings on peanut-shell–reinforced composites, where moderate filler loading significantly improved tensile strength compared to untreated or higher filler loadings [8]. The decline in tensile strength for Samples D (14.70 N/mm^2) and E

(14.93 N/mm²) at 40g and 50g loadings suggests filler agglomeration and reduced interfacial bonding. Excessive nanofiller content can lead to particle clustering, creating stress concentration sites that weaken the composite [9].

Hardness properties

The Shore A hardness results in increase from 37.21 (Sample A) to a plateau of 56.84–58.30 for Samples C–E, a 57% improvement. This enhancement is attributed to restricted polymer chain mobility and increased crosslink density due to the presence of rigid groundnut shell nanoparticles [8]. Similar hardness improvements were observed in peanut-shell–reinforced thermoplastics, where nanofillers enhanced resistance to surface indentation [10].

Abrasion resistance performance

The abrasion resistance data showed an improvement with increasing nanofiller content, decreasing from 69.29 mm³/rev (Sample A) to 53.91 mm³/rev (Sample D). Lower values indicate better wear performance, likely due to the formation of a protective nanoparticle layer at the composite surface [8].

Compression set behavior

The compression set values drop from 46.39% for Sample A to 34.04% for Sample D, resulting in a 27% improvement, which indicates better elastic recovery and dimensional stability. This implies that nanofillers from groundnut shells reinforce the crosslink network, minimizing permanent deformation when subjected to compressive loads [8].

Flex fatigue performance

The flex fatigue test evaluates the resistance of composites to repeated bending cycles. The SI unit of the count is the cycle, representing the number of flexes before crack initiation. In this study, crack initiation was observed at different cycles and times for the nanofiller-loaded samples, while Sample A (10 g) showed no cracks throughout the test duration (Table 1). The results (Figure 1) demonstrate that fatigue resistance improved with increasing nanofiller loading, with Sample E (50 g) achieving the highest performance (4,442 cycles, 75 min). This can be attributed to the reinforcing role of groundnut shell nanoparticles, which act as barriers to crack propagation and enhance stress distribution [8, 10].

Table 1: Flex Fatigue – Cycles to crack across samples B–E

Sample	Filler Loading (g)	Cycles to Crack	Time to Crack (min)
A	10	No crack	No crack
B	20	2,096	38
C	30	3,489	43
D	40	3,981	58
E	50	4,442	75

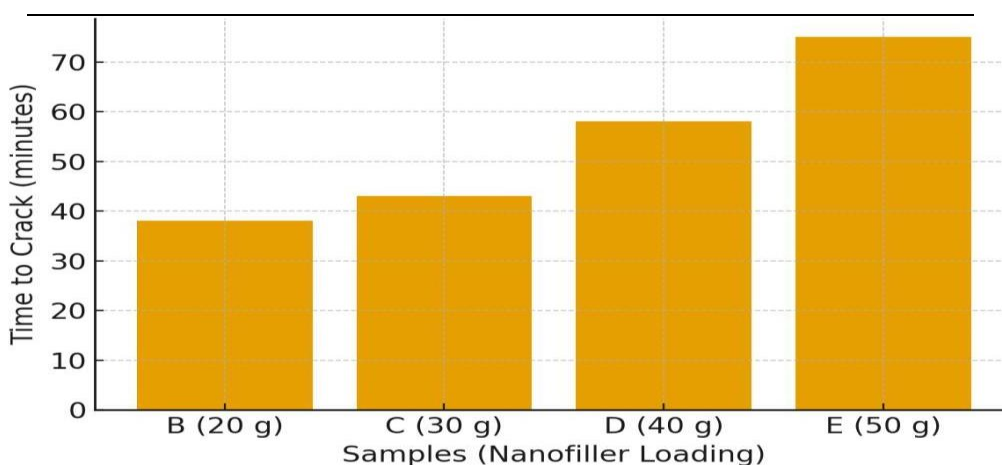


Figure 1: Flex Fatigue – Time to crack (minutes) across samples B–E.

Optimal loading determination

Based on the mechanical characterization, Sample C (30 g nanofiller loading) emerges as the optimum, delivering:

- Maximum tensile strength (15.99 N/mm²)
- Highest tensile modulus (4.75 N/mm²)
- Excellent hardness (58.30 Shore A)
- Good abrasion resistance (60.64 mm³/rev)
- Acceptable compression set (38.67%)

This mid-range filler loading aligns well with optimal concentrations in natural-filler composites, which often yield tensile strength improvements of ~25-30% [8, 10].

Reinforcement mechanisms

The composites created in this study demonstrate promise for applications in automotive interiors, building materials, packaging, and consumer products—areas where performance and sustainability intersect [10]. The formulation with a 30 g loading optimizes both mechanical performance and processability, providing a cost-efficient option for industrial use.

SEM/EDX analysis of groundnut shell-derived nanofillers

The SEM micrograph revealed spherical and elliptical voids (2-10 μm in diameter) distributed throughout the matrix, with thin, continuous pore walls forming a three-dimensional scaffold.

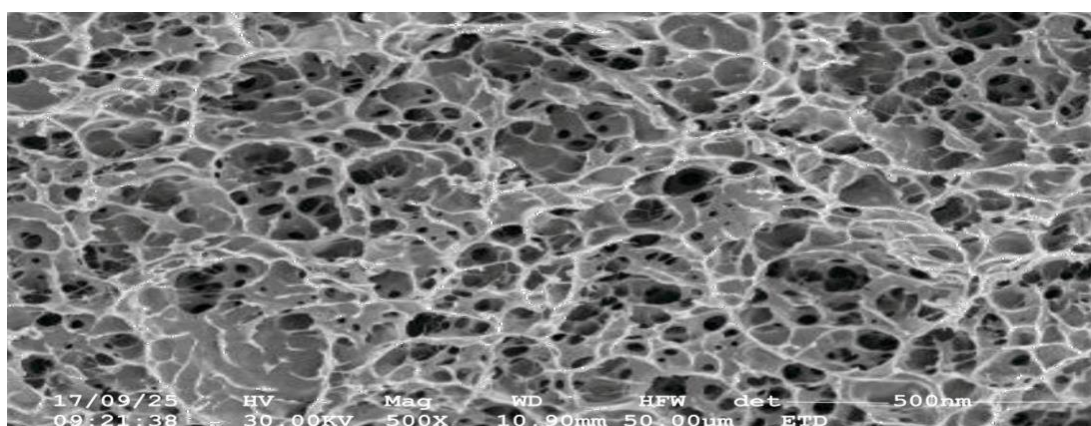


Figure 2: SEM of sample 1A

Sample 1A displayed a highly porous, interconnected foam-like structure (Figure 2). This morphology, typical of thermally treated lignocellulosic biomass, results from the release of volatile components, yielding a porous carbonaceous structure [11,12]. The porous architecture is ideal for enhancing mechanical interlocking and load transfer in polymer composites [13].

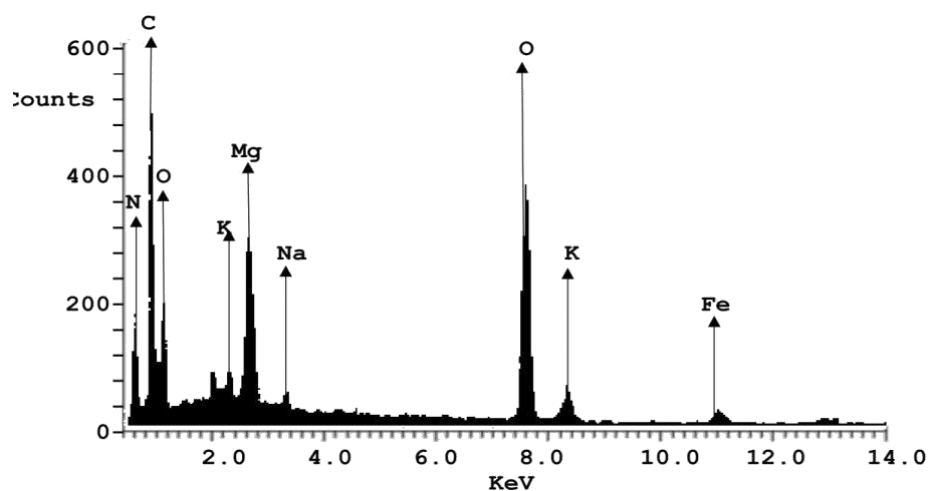


Figure 3: Elemental Composition

The prevalence of C, N, and O aligns with the lignocellulosic composition of groundnut shells (Figure 3) [14]. Mg, K, and Na reflect the mineral content typical of agricultural residues, concentrated in the ash fraction [15,16].

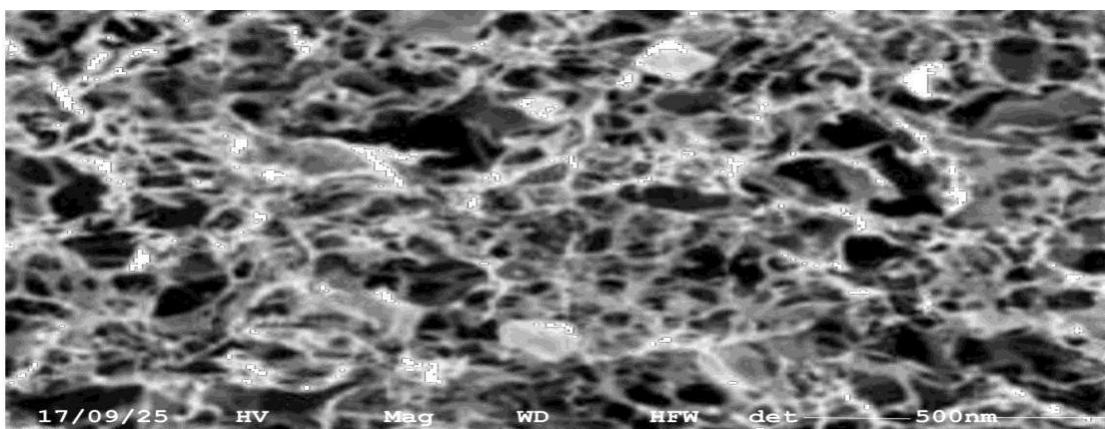


Figure 4: SEM of sample 2B

Sample 2B (Figure 4) exhibited a moderately porous structure with irregularly shaped voids (1-8 μ m) and denser regions. The micrograph showed thicker pore walls and occasional bright spots, indicating aggregates. This less uniform morphology suggests partial densification or varying processing conditions compared to Sample 1A [17].

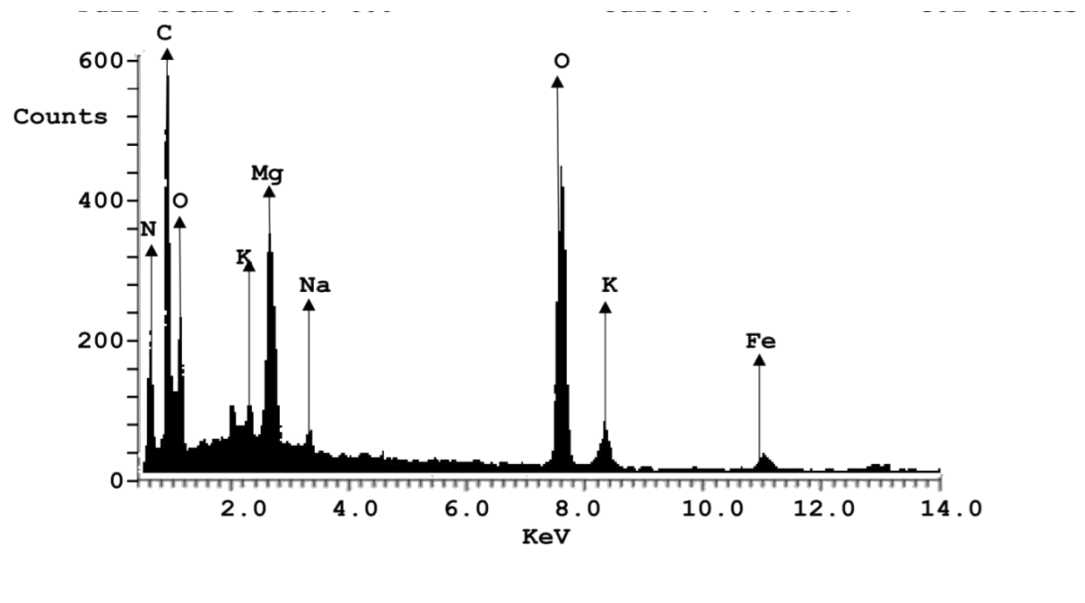


Figure 5: Elemental profile of Sample 2B

The elemental profile is nearly identical to Sample 1A, indicating similar chemical composition despite morphological differences [16]. The slightly higher count (592 vs. 584) may reflect a denser or thicker analyzed region.

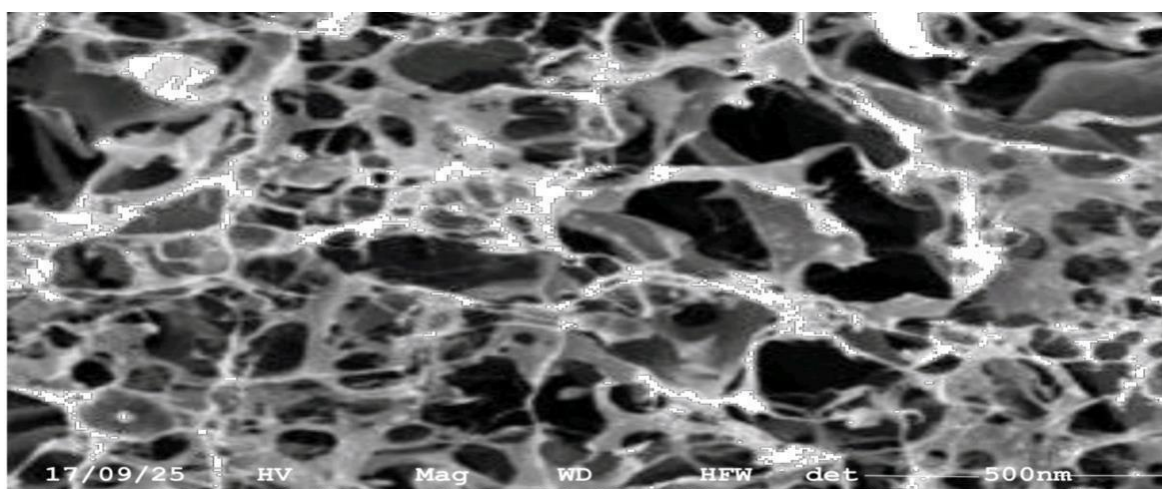


Figure 5: SEM of sample 3C

Sample 3C (Figure 5) exhibited a hierarchical porous structure featuring a bimodal pore distribution, with macropores (5-15 μm) linked by mesopores (1-3 μm). The walls of the pores had a membranous, sheet-like appearance characterized by striations. Certain areas displayed partial collapse, resulting in regions of consolidation. This structure, which is

typical of biomass-derived carbons produced through controlled pyrolysis, indicates a high surface area and accessibility, making it advantageous for use as nanofillers in polymer matrices [15, 13].

The presence of chlorine, absent in other samples, may result from natural occurrence, processing contamination, or chemical treatment [18]. The lower count (487) suggests reduced material density.

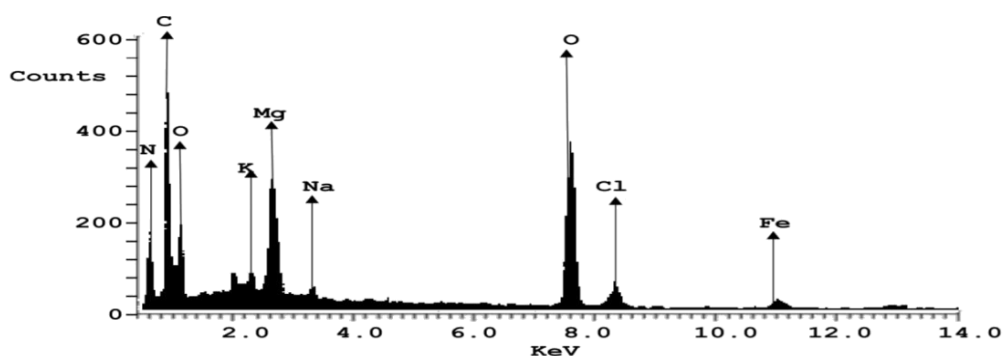


Figure 6: Elemental profile of Sample 4D

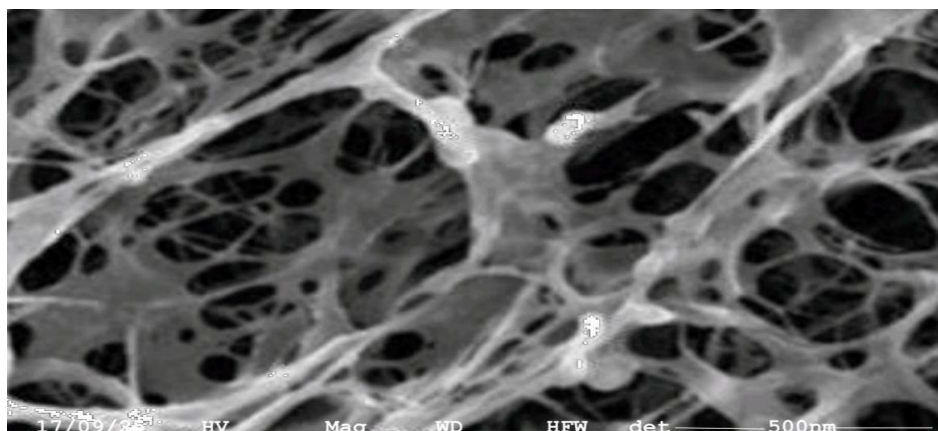


Figure 7: SEM of sample 4D

Sample 4D (Figure 7) exhibited a well-defined porous structure with elongated, elliptical voids (3-12 μm) arranged in an organized pattern. Thin interpore walls and bright spots (indicating crystalline or dense particles) were observed. This oriented morphology likely reflects the preservation of the groundnut shell's vascular structure, offering potential for directional reinforcement in composites [17, 13].

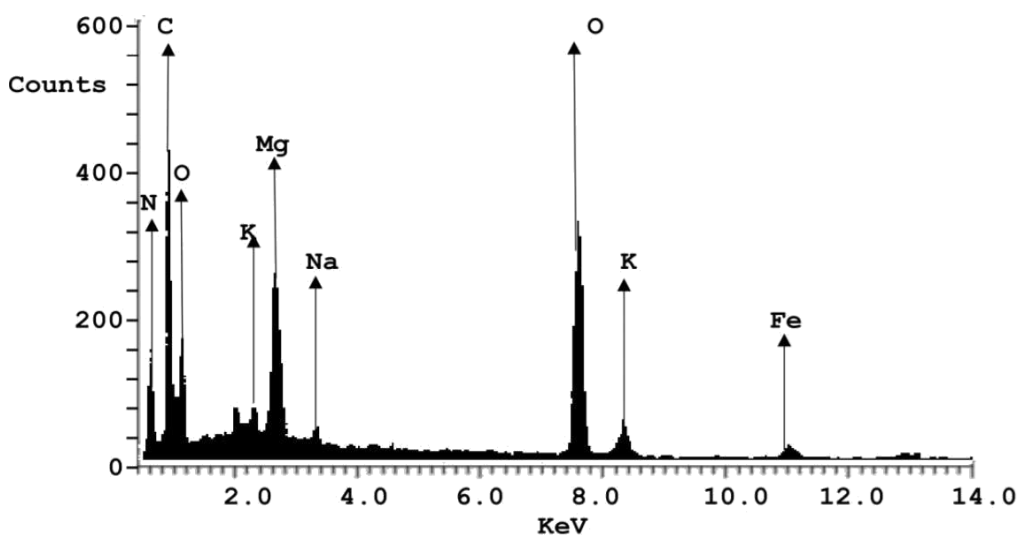


Figure 8: Elemental profile of Sample 5 E

The composition (Figure 8) mirrors Samples 1A and 2B, lacking chlorine. Morphological differences likely stem from processing rather than chemical variation [19].

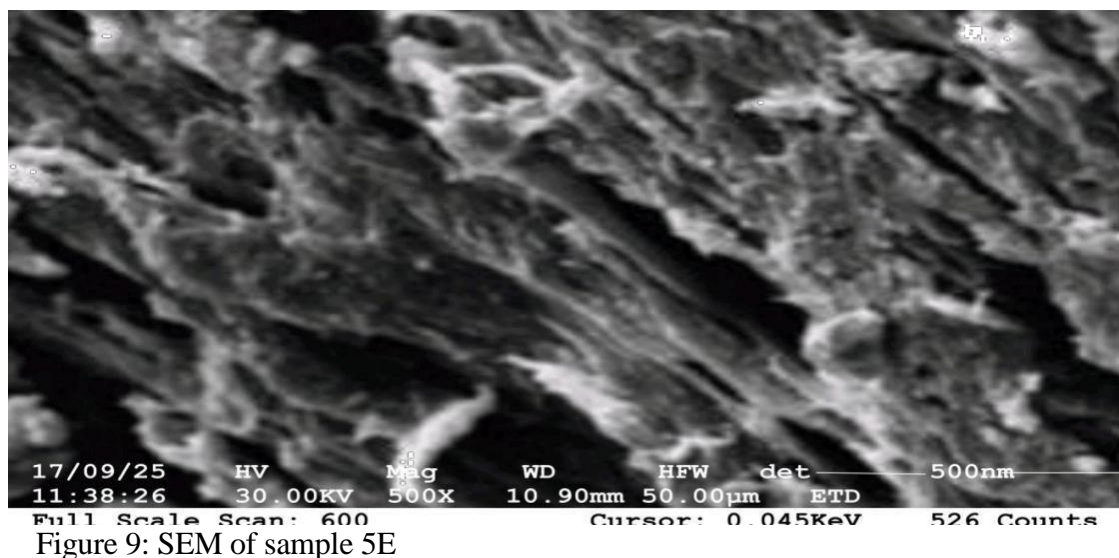


Figure 9: SEM of sample 5E

Sample 5E (Figure 9) exhibited a dense, fibrous network of elongated, rod-like elements (10-50 µm long, 0.5-2 µm wide), forming an interwoven mat. This fibrous morphology, characteristic of cellulose nanofibers, suggests mechanical or chemical treatment of lignocellulosic biomass [20,15].

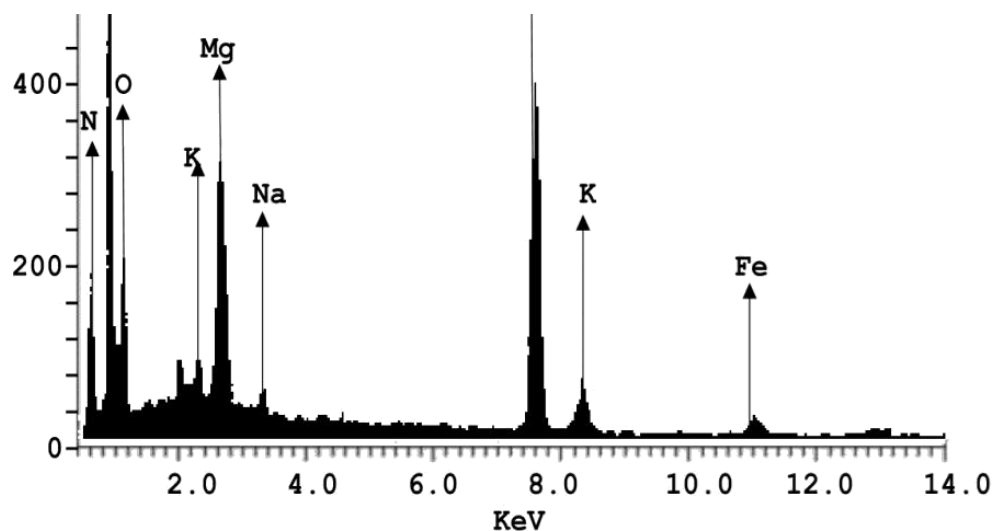


Figure 10: Elemental profile

The composition (Figure 10) aligns with Samples 1A, 2B, and 4D, with no chlorine. The intermediate count (526) indicates moderate density.

Morphological comparison

The samples displayed diverse morphologies, reflecting varied processing methods. Samples 1A, 2B, 3C, and 4D showed porous structures typical of carbonized biomass, with differences in pore size and organization [18]. Sample 5E's fibrous morphology indicates a cellulosic nanofiller, distinct from the others [21]. The range of porous structures (from uniform foam-like in 1A to oriented pores in 4D) highlights the influence of thermal processing, while Sample 5E's fibrous form suggests mechanical or chemical extraction [17].

Elemental composition comparison

All samples shared a consistent elemental profile (C, N, O, Mg, K, Na, Fe), reflecting their lignocellulosic origin [14]. Sample 3C's unique chlorine peak may indicate processing or environmental factors [19]. Count variations (584-592 for 1A and 2B, 487 for 3C and 4D, 526 for 5E) suggest differences in density or surface composition [16].

Structure-composition relationship

Despite morphological diversity, the consistent elemental composition indicates that processing parameters, not starting material, drive structural differences [17]. Porous structures (1A-4D) result

from carbonization, while fibrous Sample 5E reflects cellulose extraction [19]. This versatility allows groundnut shells to be tailored for various composite applications [20].

FTIR spectroscopic analysis of groundnut shell nanofiller for polymer composite applications

The FTIR spectrum of groundnut shell nanofiller reveals key absorption bands that confirm its lignocellulosic composition, making it a promising reinforcement material for polymer composites. A broad, intense peak at 3411.23 cm^{-1} corresponds to O-H stretching vibrations, indicating hydroxyl groups in cellulose and hemicellulose, which facilitate hydrogen bonding and enhance interfacial interactions with polymer matrices. This is consistent with findings by Popescu et al. [22] and Dhinakarraaj et al. [23]. The peak's breadth reflects diverse hydroxyl environments, including free and hydrogen-bonded OH groups typical of lignocellulosic materials. Additionally, peaks at 2919.46 cm^{-1} and 2897.10 cm^{-1} arise from asymmetric and symmetric C-H stretching of methyl and methylene groups in cellulose and hemicellulose, contributing to the nanofiller's hydrophobic character and influencing compatibility with polymer matrices, as noted by Usman et al. [11]. Moreover, a peak at 2250.19 cm^{-1} suggests $\text{C}\equiv\text{C}$ or $\text{C}\equiv\text{N}$ stretching, likely from lignin's aromatic or nitrile functionalities, enhancing mechanical strength and thermal stability critical for composite reinforcement. This aligns with findings by Sharma & Vuppu [19]. Bands at 1421.65 cm^{-1} and 1386.41 cm^{-1} correspond to C-H bending and CH_2 wagging in cellulose and hemicellulose, with the former linked to cellulose's crystalline regions, confirming the nanofiller's structural integrity for mechanical reinforcement, as reported by Usman et al. [11]. A prominent peak at 1050.28 cm^{-1} , attributed to C-O stretching in cellulose's pyranose ring and C-O-C glycosidic linkages, verifies high cellulose content essential for composite applications, consistent with findings by Bastian et al. [25]. Furthermore, peaks at 986.14 cm^{-1} and 891.24 cm^{-1} reflect C-C stretching and out-of-plane C-H bending, linked to β -glycosidic linkages in cellulose and aromatic C-H in lignin, while the 550.32 cm^{-1} band indicates skeletal vibrations, supporting the lignocellulosic framework. The FTIR analysis confirms that the nanofiller retains critical lignocellulosic components, including hydroxyl groups for interfacial bonding, a cellulosic backbone for mechanical strength, and lignin-derived aromatic structures for thermal stability, positioning it as an effective, sustainable reinforcement for polymer composites with enhanced mechanical and thermal properties.

X-Ray diffraction analysis

X-ray diffraction analysis was performed to determine the crystallographic structure and assess the crystallinity of the synthesized material. The diffractogram obtained from sample is presented in Figure 11, showing the relationship between diffraction intensity (arbitrary units) and diffraction angle (2θ) over a scan range of 10° to 70° .

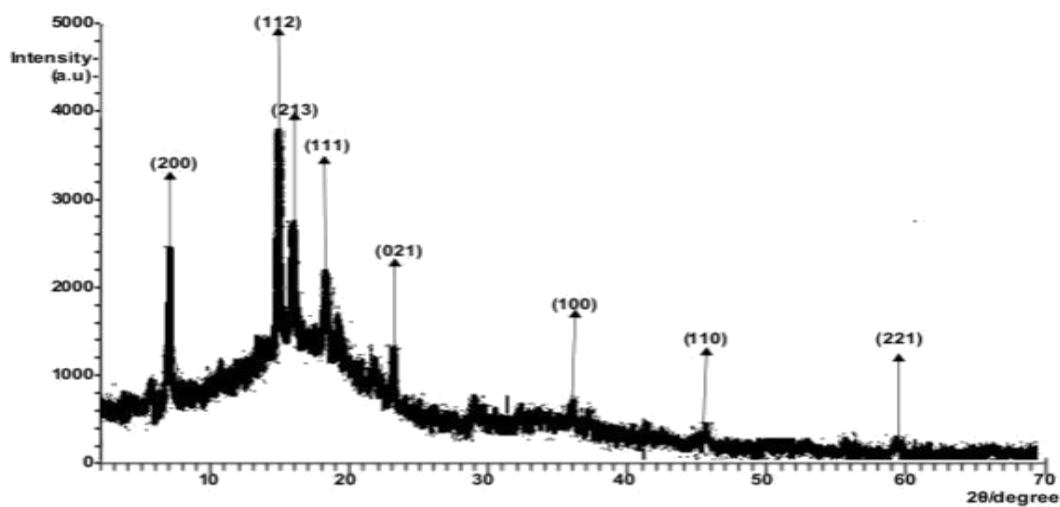


Figure 11: XRD spectrum diagram

Diffraction pattern and peak identification

The XRD pattern revealed multiple sharp, well-defined diffraction peaks, indicating a highly crystalline material with excellent long-range atomic order. Eight distinct peaks were identified and indexed according to their corresponding miller indices (hkl), which represent the crystallographic planes responsible for the diffraction. The observed peaks occurred at the following approximate 2θ positions: (100) at $\sim 18^\circ$, (110) at $\sim 23^\circ$, (111) at $\sim 28^\circ$, (200) at $\sim 32^\circ$, (021) at $\sim 38^\circ$, (112) at $\sim 43^\circ$, (213) at $\sim 48^\circ$, and (221) at $\sim 58^\circ$.

The most intense peak was observed for the (112) plane at approximately $2\theta = 43^\circ$, reaching a maximum intensity of 5000 arbitrary units. This dominant reflection suggests preferential crystal orientation along the (112) direction, which may result from the synthesis conditions or sample preparation method [27]. The high intensity of this peak relative to others in the pattern indicates that a significant proportion of crystallites are oriented with their (112) planes parallel to the sample surface.

Crystallinity and structural quality

The XRD analysis confirmed the successful synthesis of a highly crystalline material with well-defined crystallographic structure, as evidenced by sharp diffraction peaks and low background noise. The dominant (112) reflection and the systematic appearance of indexed peaks demonstrate excellent structural order suitable for detailed characterization and application development.

CONCLUSION

This study effectively showed that adding nanofillers derived from groundnut shells to polymer matrices significantly improves their mechanical and structural characteristics. The research concludes that an optimal loading of 30 g of nanofiller yields the best combination of tensile strength, hardness, abrasion resistance, and elastic recovery. When the filler loading exceeds 40 g, agglomeration occurs, which undermines interfacial bonding and diminishes the performance of the composite. FTIR and SEM/EDX analyses confirm that the nanofillers maintain the necessary lignocellulosic characteristics and porous structure that are crucial for effective mechanical reinforcement. XRD analysis indicates a high degree of crystallinity, reflecting enhanced structural order and mechanical strength. The interplay between morphological structure, chemical composition, and mechanical response supports the utilization of groundnut shell nanofillers in applications such as automotive interiors, construction panels, packaging, and consumer goods, where both performance and sustainability are vital. The findings affirm that agricultural waste such as groundnut shells can serve as a sustainable raw material for advanced polymer composite development, supporting both environmental protection and material innovation.

REFERENCES

- [1] Faruk, O., Bledzki, A. K., Fink, H.-P. & Sain, M. (2012). Biocomposites reinforced with natural fibers: 2000–2010. *Progress in Polymer Science*, 37(11), 1552–1596.
- [2] Wypych, G. (2016). Handbook of Fillers. ChemTec Publishing. 4th edition.
- [3] Renu Singh., Ruma Das., Seema Sangwan., Bharti Rohatgi., Rubina Khanam., S. K. Pedda Ghouse Peera., Shrila Das., Yvonne Angel Lyngdoh., Sapna Langyan., Ashish Shukla., Manoj Shrivastava & Shivdhar Misra (2021). Utilisation of agro-industrial waste for sustainable green production: A review. *Environmental Sustainability*. <https://doi.org/10.1007/s42398-021-00200-x>.

- [4] Mohanty, A. K., Vivekanandhan, S., Pin, J.-M. & Misra, M. (2018). Composites from renewable and sustainable resources: Challenges and innovations. *Science*. 362, (6414), 536-542. DOI: 10.1126/science.aat9072.
- [5] Hassan El-Ramady., Ahmed El-Henawy., Megahed Amer., Alaa El-Dein Omara., Tamer Elsakhawy., Heba Elbasiouny., Fathy Elbehiry., Doaa Abou Elyazid & Mohammed El-Mahrouk (2020). Agricultural Waste and its Nano-Management: Mini Review. *Egypt Journal of Soil Science*. 60(4), 349-364. <http://ejss.journals.ekb.eg/>
- [6] Jumaidin, R., Sapuan., S. M., Jawaid., M, Ishak, M. R. & Sahari, J. (2017). Effect of seaweed on mechanical, thermal, and biodegradation properties of thermoplastic sugar palm starch/agar composites. *International Journal of Biological Macromolecules* 99, 265-273.
- [7] Zahra Moazzami Goudarzi. & Sohrab Asgaranb (2024). The emerging role of bio-based nanocomposites in sustainable engineering applications: Current progress and future directions. *Journal of Composites and Compounds* 6(2024) 1-2.
- [8] Mandala, R., Hegde, G., Kodali, D. & Kode, V. R. (2023). From waste to strength: Unveiling the mechanical properties of peanut-shell-based polymer composites. *Journal of Composites Science*, 7(8), 307. <https://doi.org/10.3390/jcs7080307>.
- [9] Kuan, H. T. N., Tan, M. Y., Shen, Y. & Yahya, M. Y. (2021). Mechanical properties of particulate organic natural filler-reinforced polymer composite: A review. *Composites and Advanced Materials*, 30, 1–14. <https://doi.org/10.1177/26349833211007502>.
- [10] Zaaba, N. F. & Ismail, H. (2018). A review on peanut shell powder reinforced polymer composites. *Polymer-Plastics Technology and Engineering*, 58(4), 349-365. <https://doi.org/10.1080/03602559.2018.1471720>.
- [11] M. Usman., I & Momohimoh A Gimba (2016). Effect of groundnut shell powder on the mechanical properties of recycled polyethylene and its biodegradability. *Journal of Minerals and Materials characterization and Engineering*. DOI:10.4236/JMMCE.2016.43021, Corpus ID: 54702516.
- [12] Thakur, V. K. & Thakur, M. K. (2014). Processing and characterization of natural cellulose fibers/thermoset polymer composites. *Carbohydrate Polymers*, 109, 102–117. <https://doi.org/10.1016/j.carbpol.2014.03.039>.

- [13] Panel Yingji Wu., Changlei Xia., Liping Cai., Andres C. Garcia ., Sheldon Q. Shi (2018). Development of natural fiber-reinforced composite with comparable mechanical properties and reduced energy consumption and environmental impacts for replacing automotive glass-fiber sheet molding compound. *Journal of Cleaner Production*, 184 (92-10). <https://doi.org/10.1016/j.jclepro.2018.02.257>.
- [14] Mohammed Awwalu Usman & Ibrahim Momohjimoh. (2018). Characterization of groundnut shell powder as a potential reinforcement for biocomposites. *Polymers from Renewable Resources*, 12, (3-4). <https://doi.org/10.1177/20412479211008761>.
- [15] Essabir, H., Nekhlaoui, S., Malha, M., Bensalah, M. O., Arrakhiz, F. Z., Qaiss, A. & Bouhfid, R. (2013). Bio-composites based on polypropylene reinforced with almond shells particles: Mechanical and thermal properties. *Materials & Design*, 51, 225–230. <https://doi.org/10.1016/j.matdes.2013.04.031>.
- [16] Vinod, A., Sanjay, M. R., Suchart, S. & Jyotishkumar, P. (2020). Renewable and sustainable biobased materials: An assessment on biofibers, biofilms, biopolymers and biocomposites. *Journal of Cleaner Production*, 258, 120978. <https://doi.org/10.1016/j.jclepro.2020.120978>.
- [17] Chandrasekar, M., Ishak, M. R., Sapuan, S. M., Leman, Z. & Jawaid, M. (2017). A review on the characterisation of natural fibres and their composites after alkali treatment and water absorption. *Plastics, Rubber and Composites*, 46(3), 119–136. <https://doi.org/10.1080/14658011.2017.1298550>.
- [18] Mittal, G., Rhee, K. Y., Mišković-Stanković, V. & Hui, D. (2016). Reinforcements in multi-scale polymer composites: Processing, properties, and applications. *Composites Part B: Engineering*, 138, 122–139. <https://doi.org/10.1016/j.compositesb.2017.11.028>
- [19] Sandeep Sharma, Bandana Kumari Sahu, Lidong Cao, Pulkit Bindra Kaur, Mahima Chaudel, Nikhil Kora Tkar, Qiliang Huang & Vijayakumar (2021). Porous nanomaterials: Main vein of agricultural nanotechnology. *Progress in materials Science* Volume 121. <https://doi.org/10.1016/j.pmatsci.2021.100812>.
- [20] Gurunathan, T., Mohanty, S. & Nayak, S. K. (2015). A review of the recent developments in biocomposites based on natural fibres and their application perspectives. *Composites Part A: Applied Science and Manufacturing*, 77, 1–25. <https://doi.org/10.1016/j.compositesa.2015.06.007>.

- [21] Sanjay, M. R., Madhu, P., Jawaid, M., Sentharamkannan, P., Senthil, S. & Pradeep, S. (2018). Characterization and properties of natural fiber polymer composites: A comprehensive review. *Journal of Cleaner Production*, 172, 566–581. <https://doi.org/10.1016/j.jclepro.2017.10.101>.
- [22] Popescu, C. M., Hill, C. A. & Curling, S. (2023). Determination of lignin, cellulose, and hemicellulose in plant materials by FTIR spectroscopy. *Journal of Analytical Chemistry*, 78(4), 414-421.
- [23] Dhinakarraj, C., Selvaraj, R. & Kumar, S. (2022). Enhanced natural fiber-based polymeric composites with biochar filler particles derived from groundnut shell biomass waste. *Biomass Conversion and Biorefinery*, 17(8), 2845-2858.
- [24] Nikita Sharma & Suneetha Vuppu (2025). A sustainable approach for conversion of leather trimming wastes into non-edible gelatine and its physicochemical analysis, optimization, FTIR, XRD characterization, and statistical study. *Biomass conversion and bio refinery*, 15, 30293-30312.
- [25] Bastian Arifin, Sri Aprilia., Pocut Nurul Alam., Farid Mulana., Amri Amin., Dilla Mars Anask & Dwita Eka Putri (2018). Characterization Nanofillers from Agriculture Waste for Polymer Nanocomposites Reinforcement. *MATEC Web of Conferences* 156, 0502. <https://doi.org/10.1051/mateconf/20181560502>.
- [26] Cullity, B. D. & Stock, S. R. (2001). *Elements of X-ray diffraction* (3rd ed.). Prentice Hall, Upper Saddle River.